Electronic Supplementary Information

Adsorptive removal of p-nitrophenol from water with mechano-synthesized porous organic polymers

Heng Zeng,[a] Weigang Lu,*[a,c] Leiduan Hao,[b] Gregory L. Helms[b], Qiang Zhang*[b] and Zhiping Luo[c]

[a] College of Chemistry and Materials Science, Jinan University, Guangzhou, Guangdong, 510632, P. R. China.

Email: weiganglu@jnu.edu.cn

[b] Department of Chemistry, Washing State University, Pullman, Washington, 99164, USA.

Email: q.zhang@wsu.edu

[c] Research and Technology Transfer Office, Fayetteville State University, Fayetteville, NC 28301, USA.

Table S1. Calculated surface areas and pore volumes for MPOP-1 to -5

Materials	BET surface area (m^2/g)	Langmuir surface area (m^2/g)	Pore volume (cm^3/g)
MPOP-1	374	591	0.25
MPOP-2	71	212	0.14
MPOP-3	556	842	0.38
MPOP-4	375	560	0.21
MPOP-5	129	234	0.14

Table S2. Residue Fe and Cl in MPOP-1 to -5, measured by Wavelength-Dispersive X-Ray Spectroscopy on JEOL JXA-8530F Hyperprobe Electron Probe Microanalyzer (EPMA)

Elements%	MPOP-1	MPOP-2	MPOP-3	MPOP-4	MPOP-5
Fe%	0.178	0.622	0.786	0.423	0.799
Cl%	0.119	0.272	0.410	1.078	0.354
Total%	0.297	0.894	1.196	1.501	1.153

Table S3. Mass spectrometer analysis method (MRM) setup for PNP and PNC and tuned parameters for product ions

Q1 mass (m/z)	Q2 mass (m/z)	Dwell time (ms)	Parameters		
			Entrance Voltage	Collision Cell Lens 2	Collision Energy
140.1 (PNP)	123.1	25	26	-28	-37
	93.2	25	27	-20	-28
	65.3	25	27	-48	-38
155.8 (PNC)	139.2	25	23	-32	-18
	109.2	25	23	-28	-28
	81.2	25	24	-52	-37

Table S4. The gradient elution setup for UPLC system

Time (min)	H_2O* (%)	Acetonitrile* (%)	Flow rate (mL/min)
0	80	20	0.5
2	80	20	0.5
3	10	90	0.5
4	10	90	0.5
4.01	80	80	0.5
5	80	80	0.5

*Both H_2O and acetonitrile contain 0.1% formic acid, which facilitate ionization.

Table S5. Adsorption kinetics parameters of PNP on MPOP-1 and MPOP-3

Kinetics	Parameters	MPOP-1	MPOP-3
Pseudo–first–order kinetic	$q_{e,exp}$(mg/g)	133.10	152.51
	k_1(1/h)	1.12	1.14
	R^2	0.96741	0.88729
Pseudo–second–order kinetic	$q_{e,exp}$(mg/g)	133.10	152.51
	k_2(g/(mg·h))	0.078	0.12
	R^2	0.99748	0.99917

The Pseudo–first–order equation: $\log (q_e - q_t) = \log q_e - (k_1/2.303)t$

Pseudo–second–order equation: $t/q_t = 1/(k_2 q_e^2) + t/q_e$

where q_e and q_t (mg/g) are the adsorption amount of PNP at equilibrium and time t(h), respectively. k_1 (h^{-1}) and k_2 (g/(mg.h)) are the Pseudo–firs–order and Pseudo–second–order adsorption rate constants, respectively.

Table S6. The detailed adsorption data and calculated PNP adsorption on MPOP-1 (one set data)

Time (d)	Peak area of PNP	Peak area of PNC (IS, 50ppm)	Peak area ratio of PNP/PNC	Conc. of PNP	Absorbed PNP (out of 50 mg)	q_t (mg/g)
0.00347	681091	313141	2.17503	216.02198	6.7956	33.97802
0.00694	627592	301604	2.08085	206.57126	8.68575	43.42874
0.02083	739887	372932	1.98397	196.85033	10.62993	53.14967
0.08333	768383	411422	1.86763	185.17561	12.96488	64.82439
0.16667	736106	414553	1.77566	175.94732	14.81054	74.05268
0.25	969449	566336	1.71179	169.53819	16.09236	80.46181
1	591144	418280	1.41327	139.58335	22.08333	110.41665
2	669504	523689	1.27844	126.05327	24.78935	123.94673
5	590186	498666	1.18353	116.52966	26.69407	133.47034

Table S7. The detailed adsorption data and calculated PNP adsorption on MPOP-3 (one set data)

Time (d)	Peak area of PNP	Peak area of PNC (IS, 50ppm)	Peak area ratio of PNP/PNC	Conc. of PNP	Absorbed PNP (out of 50 mg)	q_t (mg/g)
0.00347	1.05951E6	574019	1.84578	182.98301	13.4034	67.01699
0.00694	186658	95856	1.94728	193.16788	11.36642	56.83212
0.02083	792990	438670	1.80771	179.16361	14.16728	70.83639
0.04167	307770	172932	1.77972	176.35421	14.72916	73.64579
0.125	385526	266583	1.44618	142.88499	21.423	107.11501
0.25	435518	325300	1.33882	132.11226	23.57755	117.88774
1	479663	412273	1.16346	114.51573	27.09685	135.48427

2	705398	671391	1.05065	103.19597	29.36081	146.80403
5	246792	252407	0.97775	95.88107	30.82379	154.11893

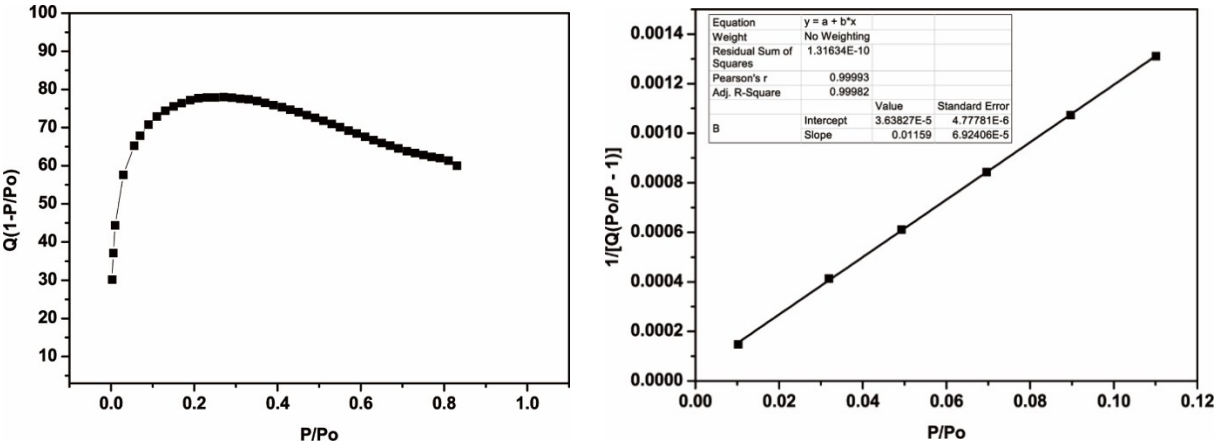

Figure S1. left) Q(1-P/Po) vs. P/Po for MPOP-1, Only the range below P/Po = 0.20 satisfies the first consistency criterion for applying the BET theory, right) Plot of the linear region for the BET equation.

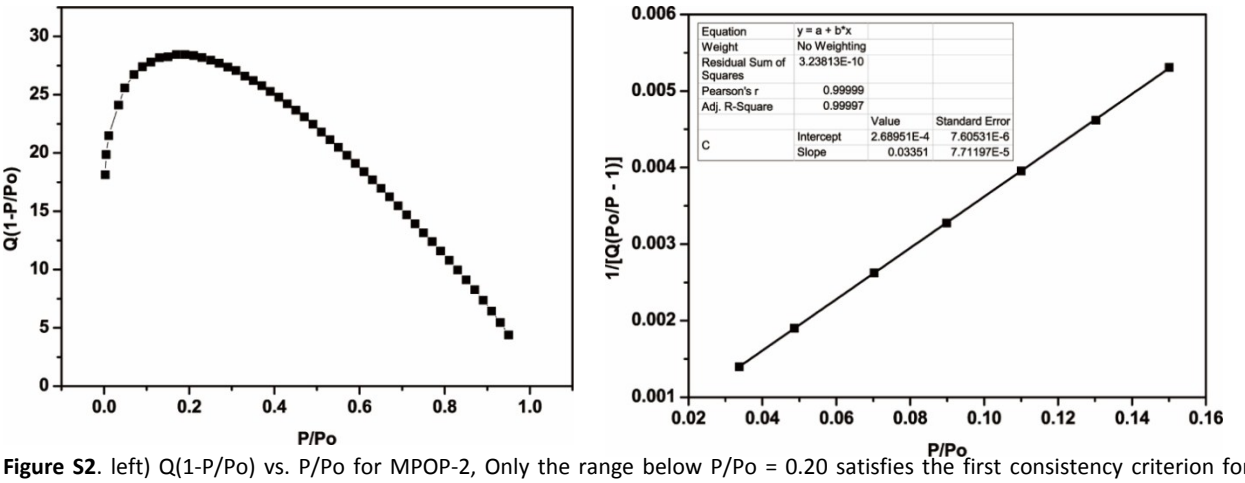

Figure S2. left) Q(1-P/Po) vs. P/Po for MPOP-2, Only the range below P/Po = 0.20 satisfies the first consistency criterion for applying the BET theory, right) Plot of the linear region for the BET equation.

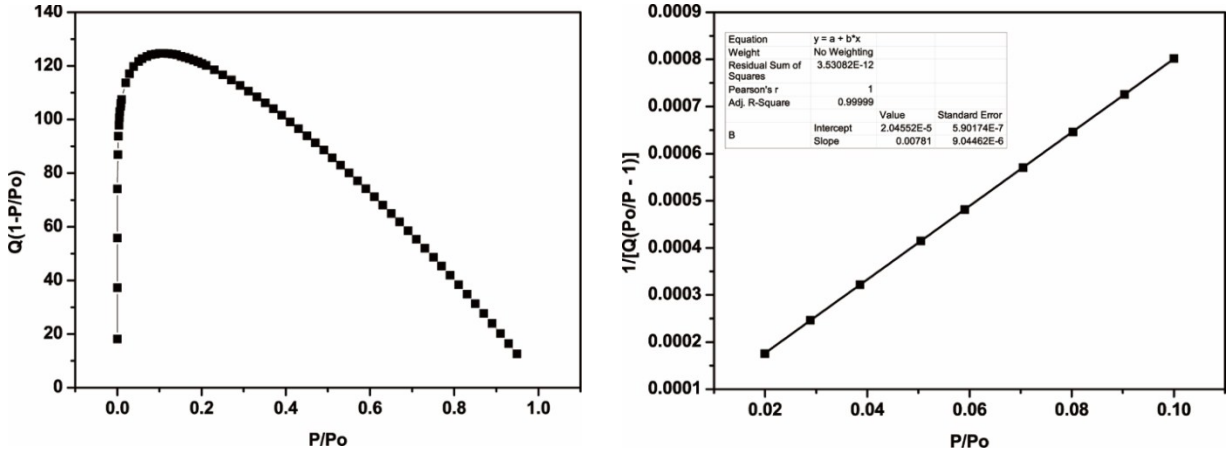

Figure S3. left) Q(1-P/Po) vs. P/Po for MPOP-3, Only the range below P/Po = 0.10 satisfies the first consistency criterion for applying the BET theory, right) Plot of the linear region for the BET equation.

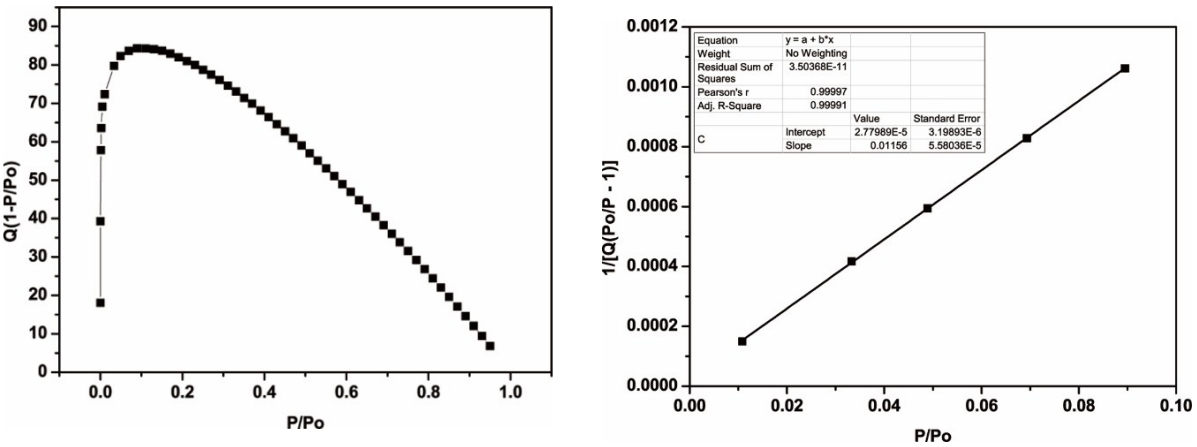

Figure S4. left) Q(1-P/Po) vs. P/Po for MPOP-4, Only the range below P/Po = 0.10 satisfies the first consistency criterion for applying the BET theory, right) Plot of the linear region for the BET equation.

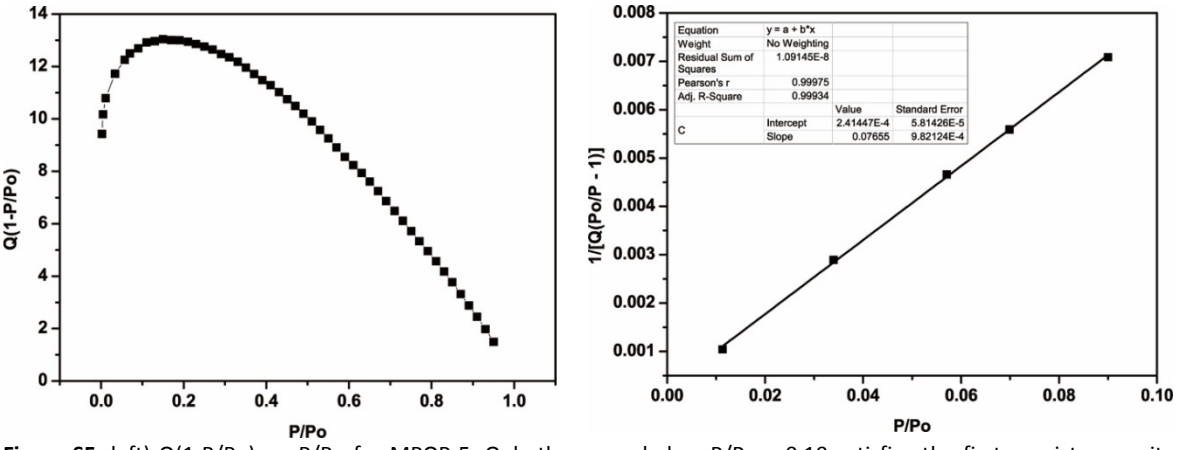

Figure S5. left) Q(1-P/Po) vs. P/Po for MPOP-5, Only the range below P/Po = 0.10 satisfies the first consistency criterion for applying the BET theory, right) Plot of the linear region for the BET equation.

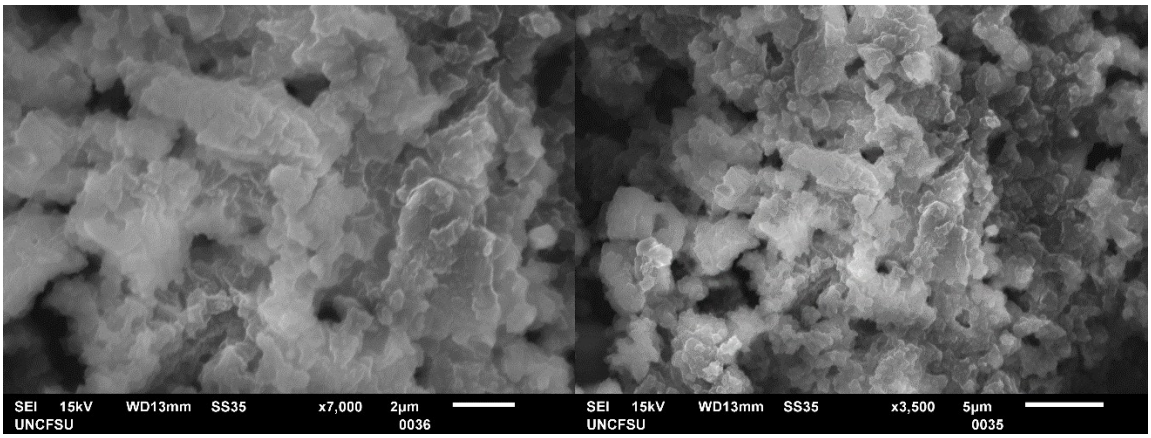

Figure S6. SEM image of MPOP-1.

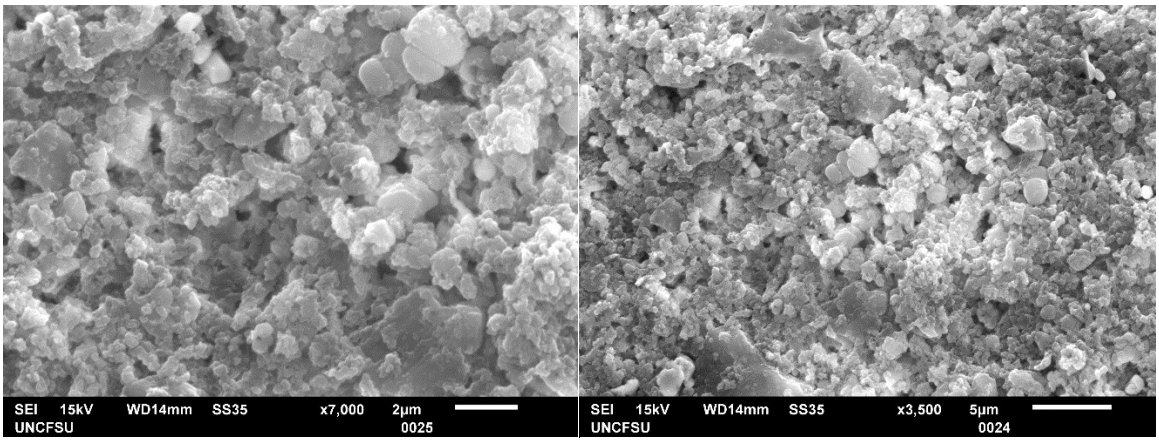

Figure S7. SEM image of MPOP-2.

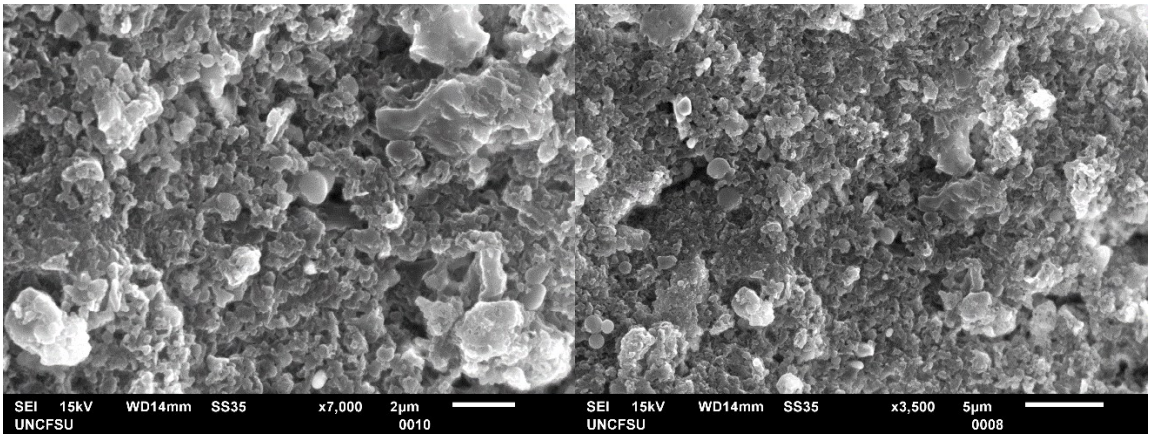

Figure S8. SEM image of MPOP-3.

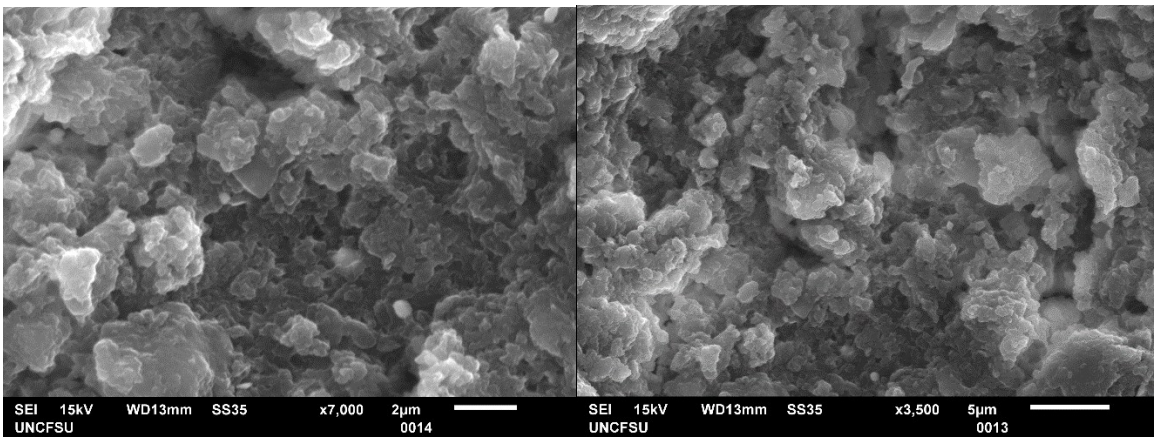

Figure S9. SEM image of MPOP-4.

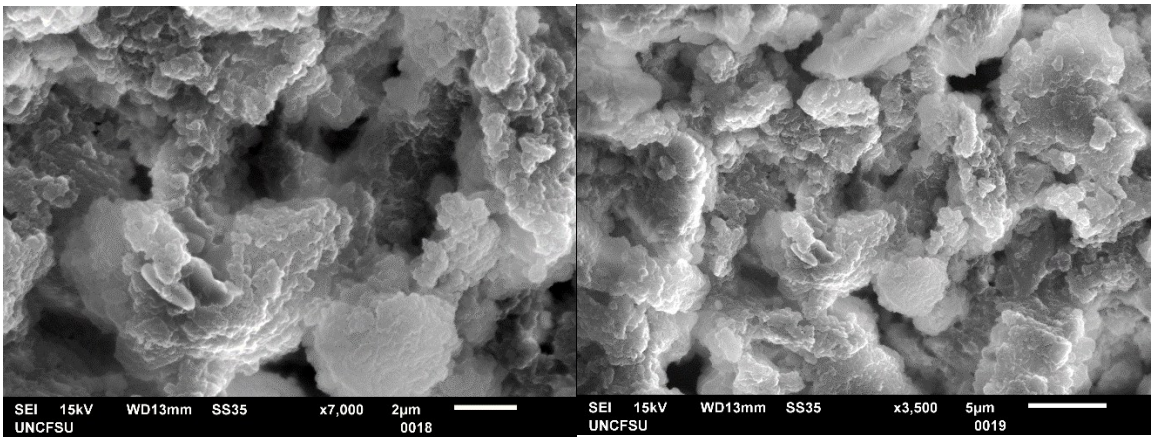

Figure S10. SEM image of MPOP-5.

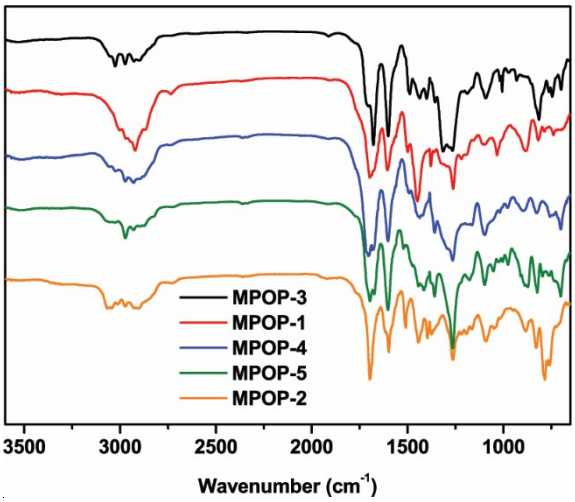

Figure S11. FT-IR spectra of MPOP-1 to -5

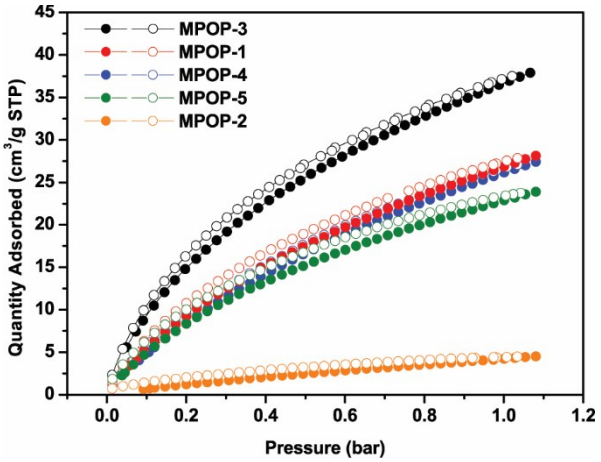

Figure S12. CO_2 adsorption (closed)/desorption (open) isotherms of MPOP-1 to -5 at 273 K.

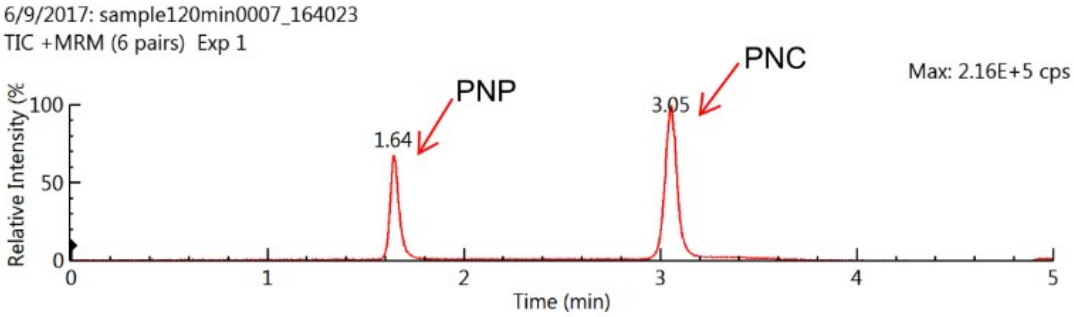

Figure S13. Total ion chromatogram for a mixed solution of PNP and PNC in a gradient elution described in **Table S4**

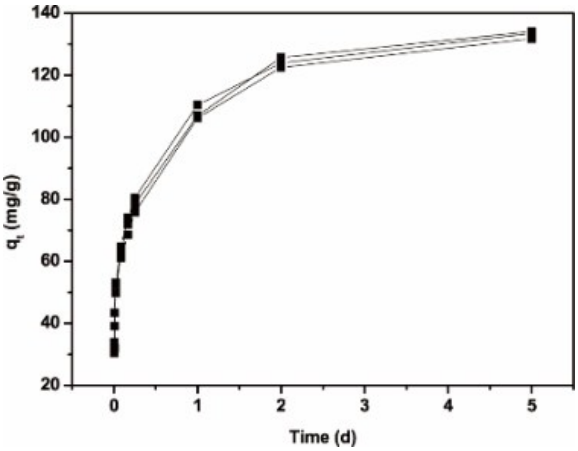

Figure S14. PNP adsorption on MPOP-1

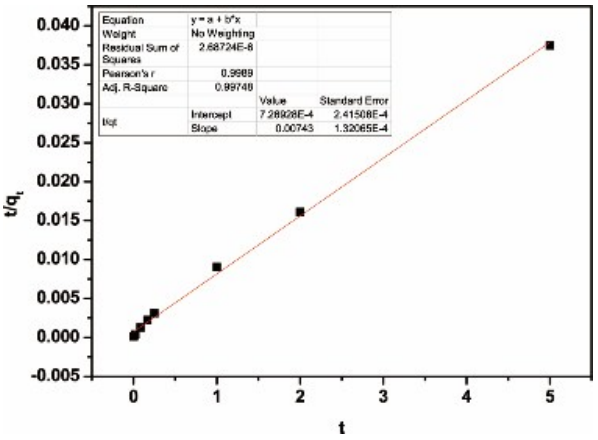

Figure S15. Pseudo–second–order plot for PNP adsorption on MPOP-1

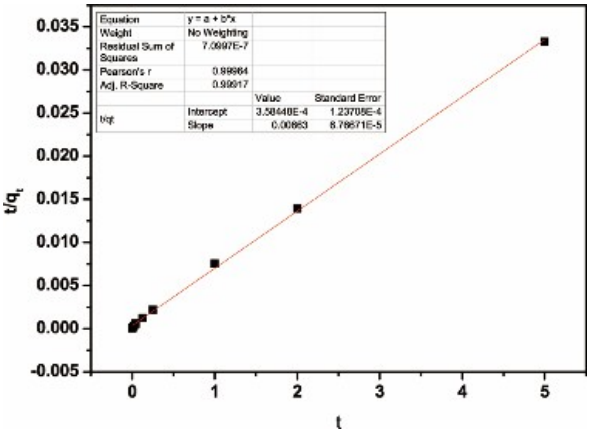

Figure S16. Pseudo-second-order plot for PNP adsorption on MPOP-3

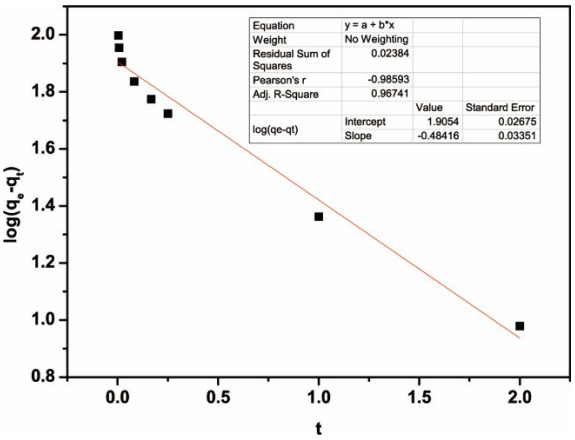

Figure S17. Pseudo-first-order plot for PNP adsorption on MPOP-1

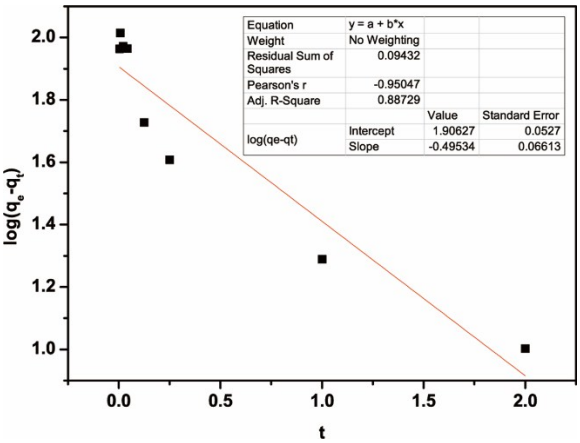

Figure S18. Pseudo-first-order plot for PNP adsorption on MPOP-3

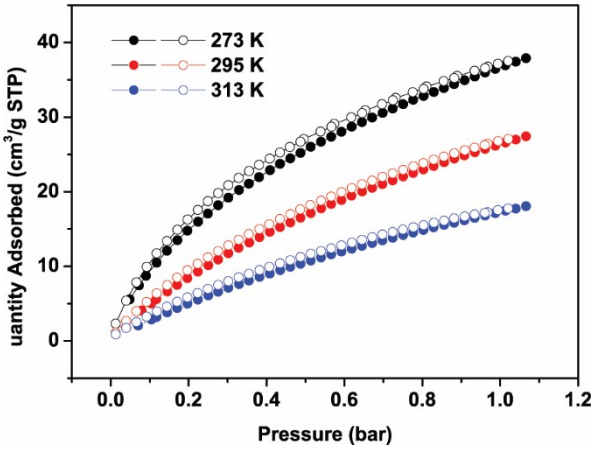

Figure S19. CO_2 adsorption (closed)/desorption (open) isotherms of MPOP-3 at different temperatures.

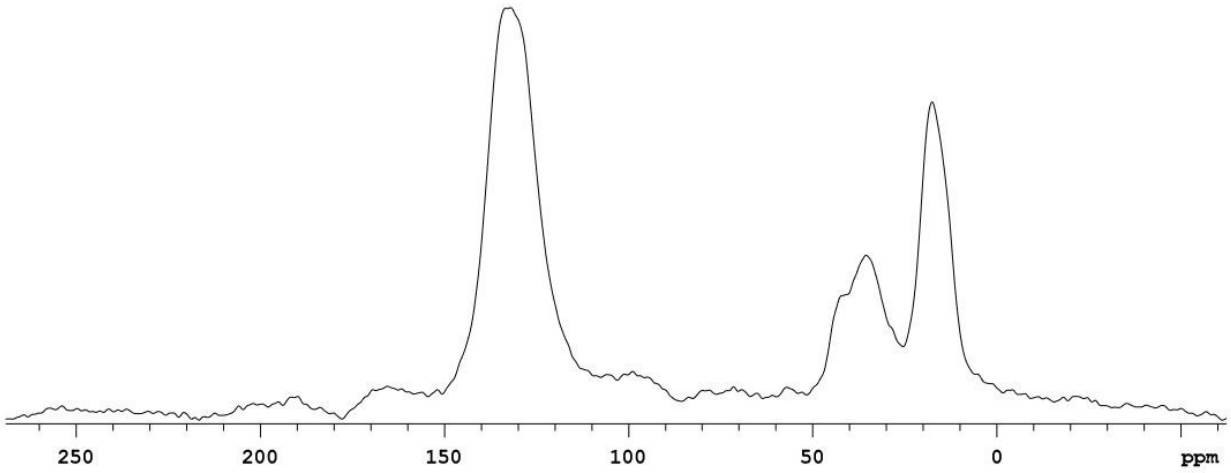

Figure S20. ^{13}C solid-state NMR for MPOP-1 (tancpxtoss, spin = 6KHz, rfl = 9410.6, rfp = 0, TOSS 4, nt = 512).

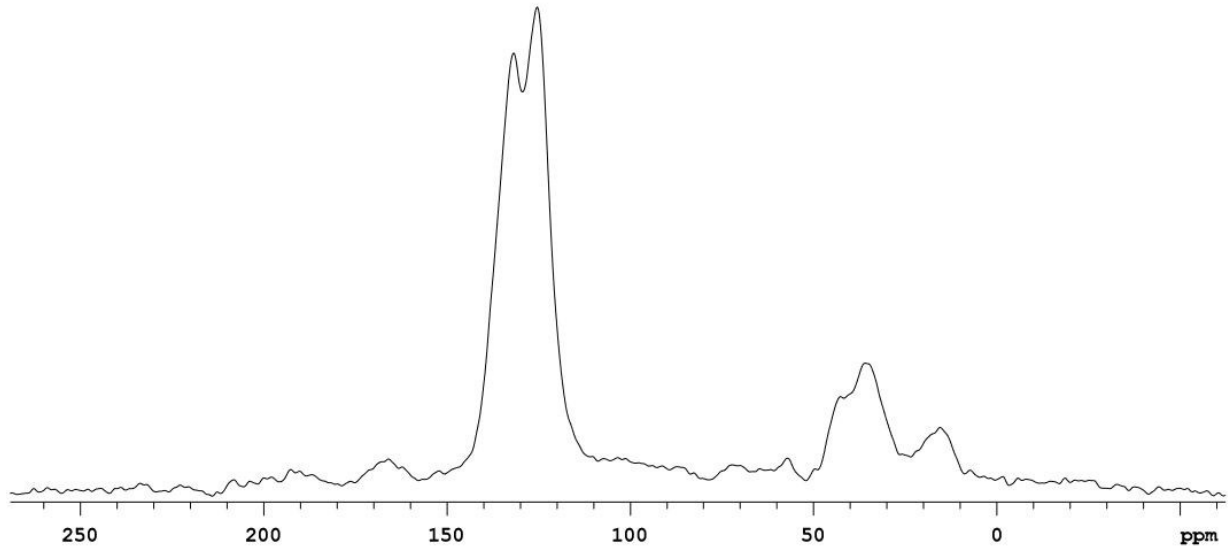

Figure S21. ^{13}C solid-state NMR for MPOP-2 (tancpxtoss, spin = 6KHz, rfl = 9410.6, rfp = 0, TOSS 4, nt = 512).

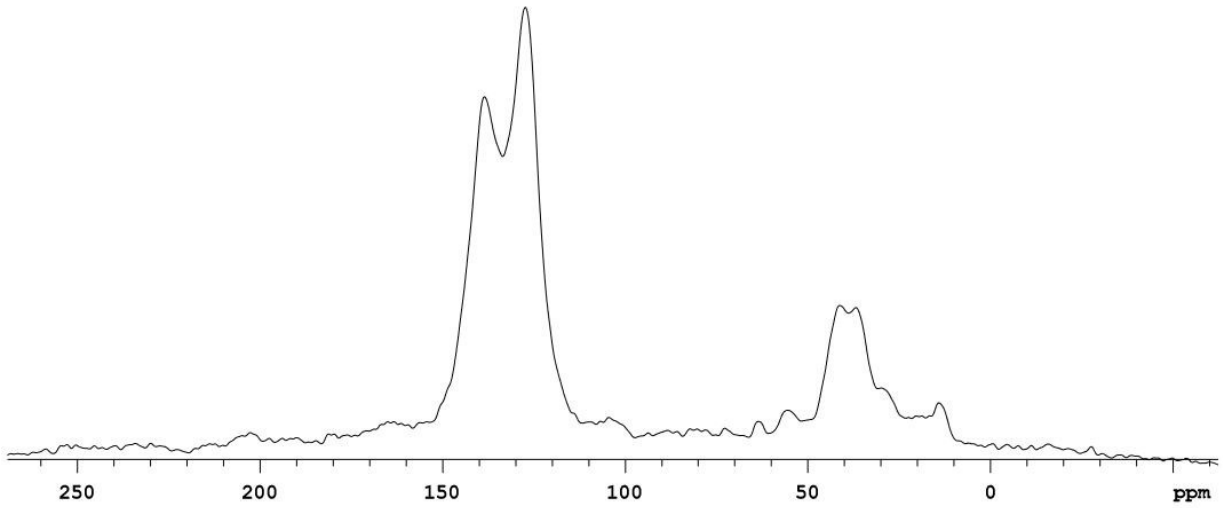

Figure S22. ^{13}C solid-state NMR for MPOP-3 (tancpxtoss, spin = 6KHz, rfl = 9410.6, rfp = 0, TOSS 4, nt = 512).

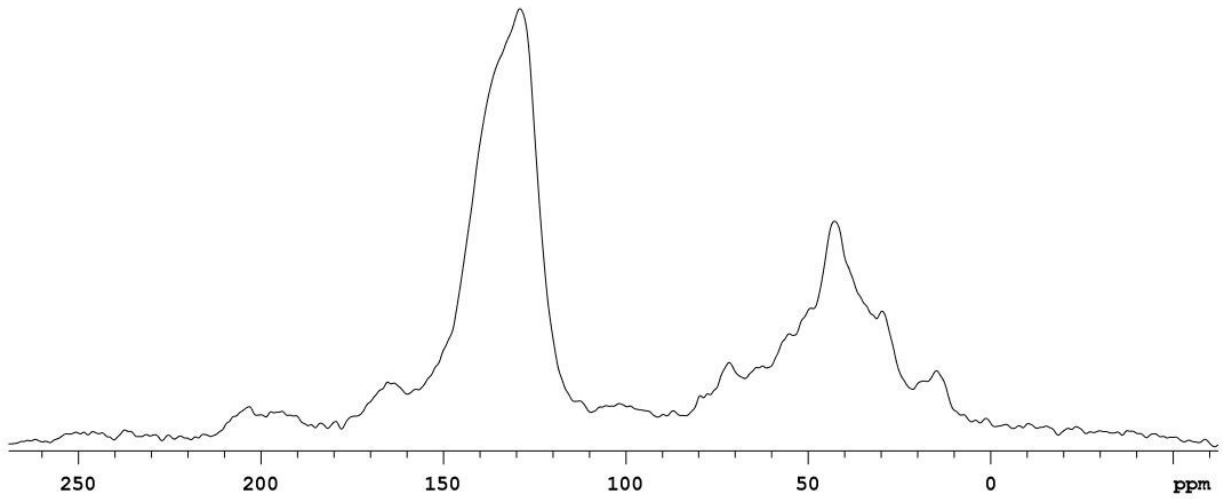

Figure S23. ^{13}C solid-state NMR for MPOP-4 (tancpxtoss, spin = 6KHz, rfl = 9410.6, rfp = 0, TOSS 4, nt = 512).

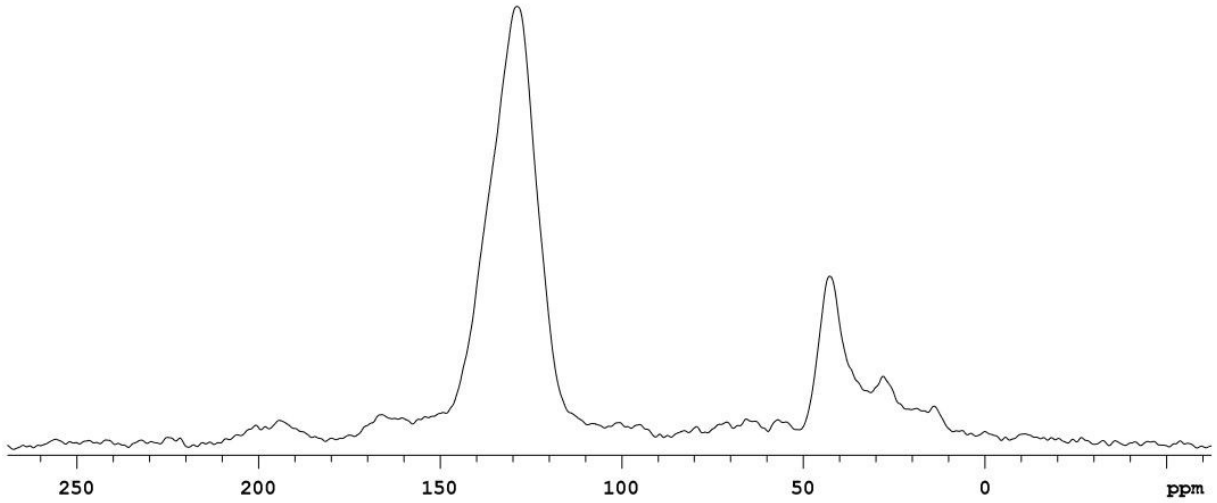

Figure S24. ^{13}C solid-state NMR for MPOP-5 (tancpxtoss, spin = 6KHz, rfl = 9410.6, rfp = 0, TOSS 4, nt = 512).

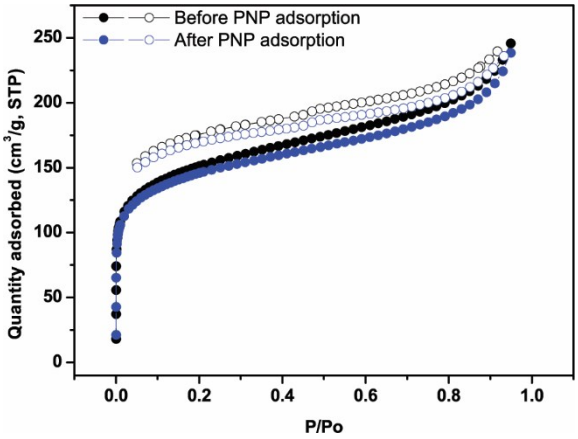

Figure S25. 77 K Nitrogen adsorption (closed)/desorption (open) isotherms of MPOP-3 before and after PNP adsorption from water.